

Options for continuous radar Earth observations

Andrea MONTI GUARNIERI* & Fabio ROCCA

*Dipartimento di Elettronica, Informazione e Bioingegneria-Politecnico di Milano,
Piazza Leonardo da Vinci, Milano 32-20133, Italy*

Received October 15, 2016; accepted January 23, 2017; published online May 24, 2017

Abstract Near Real Time (minutes or hours) radar imaging of ground targets located anywhere on an hemisphere, with or without interferometric coherence with previous passes, can be obtained with different solutions that are considered here. Geosynchronous systems, from the one proposed in 1978 by Tomiyasu to telecom satellite compatible solutions, and Low, Medium or Geosynchronous Earth Orbit constellations are discussed. Their benefits, problems, and sizes are briefly summarized, and a comparative table is presented. If interferometric coherence is requested, continuous imaging is obtained only if a very wide geostationary aperture is progressively scanned, eventually using a MIMO (Multiple Input Multiple Output) combination of several slow librating small satellites. Instead, fast librating, strip mapping, large geosynchronous satellites do provide high resolution imaging, but interferometry (and thus coherent change detection) is achievable only after a minimum delay of 12 h, i.e., when the target comes in sight without need to squint the antenna. Hence, both complex and simple systems reach full resolution interferometric imaging and thus coherent change detection capability only after 12 h.

Keywords synthetic aperture radar, continuous Earth observing system, geosynchronous systems

Citation Monti Guarnieri A, Rocca F. Options for continuous radar Earth observations. *Sci China Inf Sci*, 2017, 60(6): 060301, doi: 10.1007/s11432-016-9067-7

1 Introduction

In order to be able to monitor continuously an entire hemisphere, the instrument to be chosen is a radar, as only microwaves penetrate clouds and operate nightly. In order to achieve frequent observation, say each hour, either a rich constellation in a Low Earth Orbit (LEO) or a few satellites in Medium Earth Orbit (MEO) should be considered, or the radar should be positioned in a geosynchronous orbit, at about 36000 km from the Earth surface, or even on the moon. In this case, the extremely long distance from the target makes very large the synthetic antenna needed to achieve a reasonable azimuth resolution as well as the real antenna needed to guarantee a sufficient Signal to Noise Ratio. The synthetic antenna length is dictated by the center frequency and the resolution: for a 12.5 m resolution, the L band length is about 400 km, decreasing to about 40 km in the case of X band. This antenna is synthesized by using the relative motion of the satellite, geosynchronous but not geostationary. To add an example, from the moon a Ka band (35 GHz) SAR with 10 m resolution and 500 m² antenna would need 40 kw to make an image in just ten seconds.

* Corresponding author (email: andrea.montiguarnieri@polimi.it)

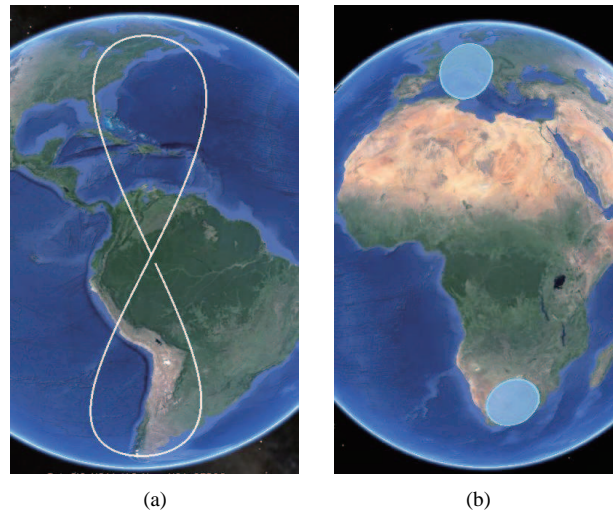


Figure 1 (Color online) (a) Nadir path of a highly inclined ($\pm 60^\circ$) geosynchronous satellite; (b) footprints of a telecom compatible geosynchronous SAR.

The fastest geosynchronous imaging system was indeed the one proposed first by Tomiyasu [1] in the late seventies. This L band system was intended for a ground range resolution of 15 m, and acted like a plane flying daily say from New York at noon to Buenos Aires at midnight and back, observing a strip about 4000 km wide (Figure 1(a)). Indeed the actual motion is enormous, but in the following we will only measure distances approximately on the nadir track.

This long trip is used to maximize the observed area and at the same time to create the ~ 50 km synthetic antenna in a time say lower than 3 min. Several other options [2–7] can be considered that take longer time to synthesize the antenna (up to hours), but then make the problem of the link budget more easily solvable, and at a lower cost, owing to the longer observation time. The several proposals made have differently inclined orbits that have nadir paths going as said from $\pm 60^\circ$ [1] to $\pm 16^\circ$, or no inclination but eccentricities with nadir paths having about the same length (a few thousand kilometers) but this time along the equator, or a combination thereof [8–10].

Taking to the extreme this kind of solution, one can consider the use of telecom satellites, that are contained in an arc of say $\pm 0.1^\circ$ (Figure 1(b)) like for the ESA Earth Explorer 9 proposal for a Geosynchronous SAR for Terrain & Atmosphere with short Revisit (GeoSTARe) [11], that in this paper we will refer to as geostationary orbit. In that case, full resolution is only obtained if using X or C bands, as the L band would have a lower resolution. The coverage can be completed by means of multiple swaths, see Figure 2. At higher frequencies, the size of the payload, the transmitted power, and the transmitting and receiving antenna reduces.

A completely different kind of solution, MIMO [12, 13], is obtained if a swarm of N geosynchronous satellites is considered, all transmitting and receiving, plus M satellites, just receiving. In that case, the aperture width is achieved instantaneously, but its spatial sampling is reduced to the $N_c = N(N + 1)/2 + MN$ phase centers that correspond to all the bistatic combinations. The satellites motion acts to fill the scan. Alternatively, LEO or MEO constellations can be considered in a polar orbit or in a nearly equatorial one. The improvement provided by a swarm is outstanding even by considering just two satellites, where three phase centers could be obtained by combining the two monostatic observation and the additional bistatic one [13].

This paper is dedicated to a comparison of the different solutions to the problem of continuous Earth observation. After the remark that objects in motion can hardly be imaged by geosynchronous systems, we will briefly recall the possible advantages of hourly observation of the terrain, and also the problems linked to the unavoidable long time needed for imaging. Namely, the effects are considered of the Atmospheric Phase Screen, of the clutter, of the interferences, and finally the link budget is sketched. After discussing the geosynchronous options we will quantify possible LEO or MEO constellations needed for a continuous

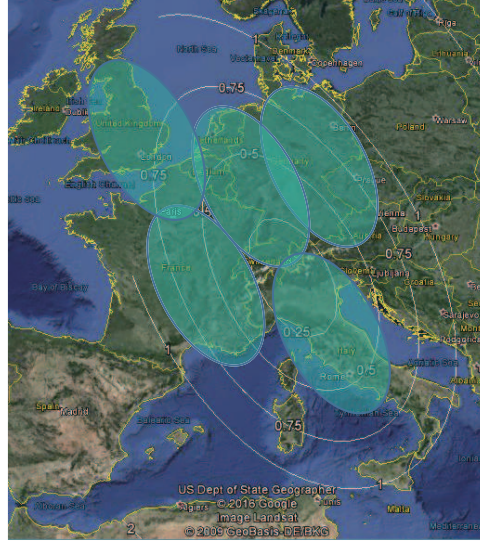


Figure 2 (Color online) Possible positions of the footprint of a C band telecom compatible SAR.

Earth observation. The conclusion will summarize the trade-offs of the different solutions.

2 Benefits and drawbacks of geosynchronous systems

In a geosynchronous SAR, the apparent velocity of the satellite with respect to Earth is much lower than in the case of Low Earth Orbits, so that the time T_{ant} needed to span the synthetic aperture, also much wider, could go from the seconds in LEO orbits to minutes and hours. Besides, the observation time T_{obs} needed to reach the desired SNR is also quite large, with respect to the usual time needed in LEO: T_{obs} is related to the link budget, and thus to the real antenna diameter and to the available power. Obviously $T_{\text{obs}} < T_{\text{ant}}$ and they coincide in the case of strip map. In the LEO case, T_{ant} is about one second, allowing imaging targets in rapid motion like ships, and even cars, as long as their motion is purely translational during this total imaging time. In the geosynchronous case, T_{ant} and T_{obs} are much longer, and may be different. The time T_{ant} increases from 2 to 3 min in the Tomiyasu solution to many hours in the GeoSTARe solution. In the case of MIMO swarms, as we shall see, $T_{\text{ant}} = 0$, but $T_{\text{obs}} > 20$ min. In fact, the full span of the synthetic antenna is immediately available, even if coarsely sampled. When T_{ant} is long, the satellite velocity v_{sat} is also low, and objects with a non-zero velocity along the line of sight v_{LOS} will shift along azimuth of the amount:

$$D = \frac{v_{\text{LOS}}}{v_{\text{sat}}} R = v_{\text{LOS}} T_{\text{eq}}, \quad T_{\text{eq}} = \frac{R}{v_{\text{sat}}}, \quad (1)$$

where R is the sensor-target distance. In (1), the azimuth shift of the moving target in the focused image, D , has been expressed as the product between the target v_{LOS} , and an equivalent time, T_{eq} . This time is quite small in LEO, about 2 min, leading to moderate shifts of moving targets (a ship travelling at 10 knots along range would be shifted less than half a km in azimuth). However, in geosynchronous SAR T_{eq} will be huge: from 6 h in the case [1], to 14 h in the case of smaller eccentricities or inclinations, and up to 120 days in the case of GeoSTARe. Due to the long time T_{ant} , be it minutes or even hours, v_{los} is also not likely to stay constant so that coherent imaging is hardly obtained. In the case of the satellite swarm $T_{\text{ant}} = 0$, and the time lapse necessary to sweep the entire antenna aperture is not devoted to increase resolution, but rather to reduce the amplitude of the replicas (due to the spatial sampling of the azimuth spectrum) imaged in the isochrona.

In substance, objects in motion are unlikely to be imaged by geosynchronous systems, even if the MIMO solution offers some hope. Nonetheless, the images of the non-moving parts of the terrain could be useful and interesting, see Figure 3. In the simulation, Billingsley ICM model has been used to evaluate the

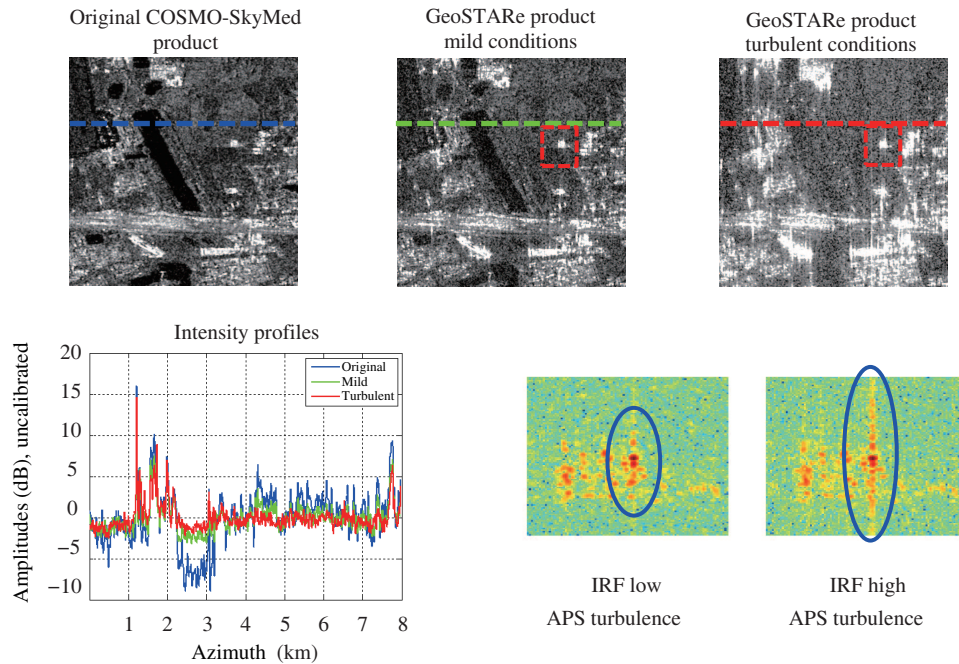


Figure 3 (Color online) End-to-end simulations of geostationary SAR products in X-band. Up left: original COSMO-SkyMed X-band image (courtesy of Agenzia Spaziale Italiana, ASI). Up middle: geostationary image at full-resolution in the case of moderate wind, and strong wind, right. Bottom left: amplitudes (vertical scale dB, uncalibrated, horizontal scale azimuth), of the iso-range cut along the dotted lines. Bottom right: zoom of a detail, from [11].

impact of X-band clutter in different wind conditions, see [14, 15], whereas the tropospheric turbulence, whose effect is observable in the partial defocusing close to point targets, was modelled as from [16].

3 Measuring precipitable water vapor and soil moisture

The benefits of a frequent observation of the terrain have been discussed in many papers [17, 18]. The foremost application could be in the evaluation of the columnar water vapor using interferometry from one pass to the next. The water vapor generates a delay that can be measured to fractions of a wavelength and therefore the additional travel path to a few millimeters. The columnar length of the Perceptible Water Vapor (PWV), about 7 times longer than the travel path [17, 19], can thus be measured with high precision and very high spatial resolution, see Figures 4 and 5. Notice that it is only possible to measure the double difference in time and space of that variable. In other words, a point in the image has to be taken as a reference, and the change of its Line Of Sight (LOS) distance with time can be related to the changes in the PWV. However, its average value in time can be determined with good precision, and therefore the initial value can be identified, also with the possible support of a high precision GPS station, co-located with any reference point in the interferogram [20–22]. As the field of view is gigantic, this is not a problem, so that we can assume that the absolute value of the PWV is gathered after a rather short observation time (say a few days, at most) in order to reach the situation when the short term average of the PWV approximates the long term one. It is important to observe that PWV is the foremost variable that has to be monitored following the criteria established by the Earth Sciences Advisory Committee (ESAC) of the European Space Agency (ESA)¹.

Notice that in order to measure the PWV, we need interferometric data, and therefore the observed span of the azimuth spectrum of the terrain has to be the same in the two images. Hence, strip map systems like [1, 9] can only observe that variable once a day whereas systems like GeoSTARe can do it continuously, as the observed azimuth spectral span is constant. We will show in next section that

1) http://m.esa.int/About_Us/ESA_Publications/ESA_Publications_Monographs/ESA_SP-1329_EO_Science_Strategy.

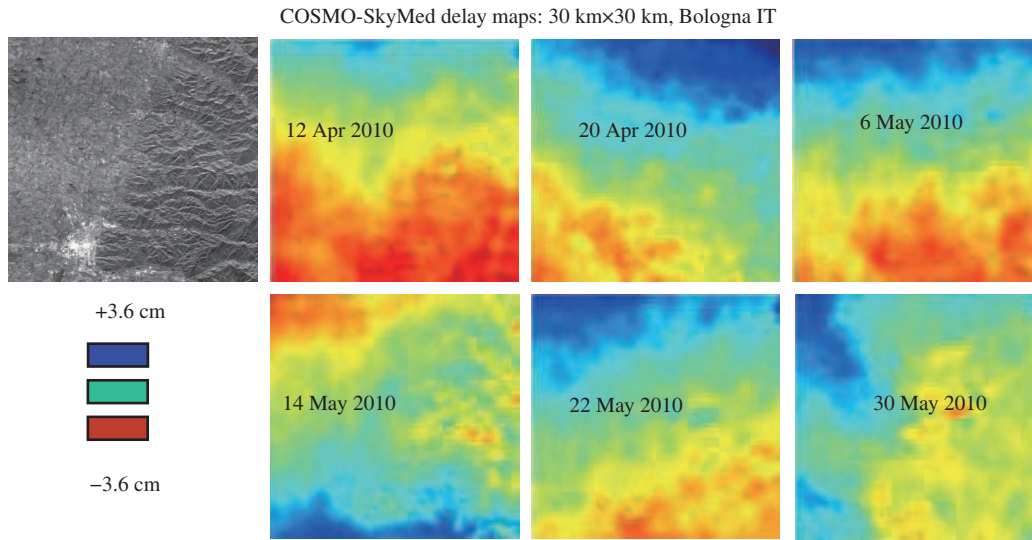


Figure 4 (Color online) Atmospheric water vapor maps over Bologna.

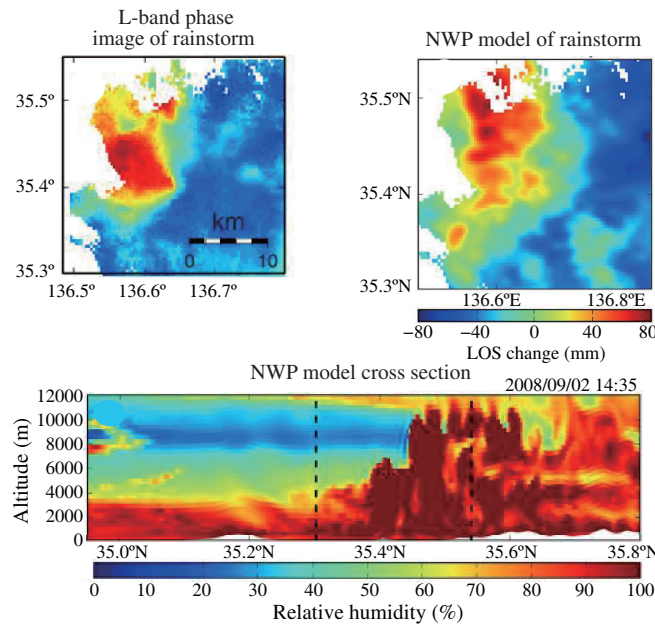


Figure 5 (Color online) Comparison between a water vapor radar map and the results of the Weather Research and Forecasting (WRF) numerical weather prediction model. In the lower part of the figure, a close up on a vertical section of the relative humidity is shown [18].

GeoSTARe has the capabilities to achieve IWV measures meeting “goal” requirements established by World Meteorological Organization (WMO), see Table 1. Currently, those requirements can be roughly achieved by infrared sensors, both polar and geostationary, only on the sea, but no sensor or combination can provide high space-time accuracy on the land.

Let us suppose that the PWV is needed in any given location in order, say, to short term forecast a local flash flood. To achieve immediately interferometry, one needs first to illuminate the area by squinting the antenna, in the case that strip mapping is used. Notice, that as the entire globe is contained in a $\pm 9^\circ$ cone if looking from a geosynchronous orbit, such a squint would be easily feasible, so that geosynchronous strip map solutions do allow continuous imaging; however, not continuous interferometric imaging. In fact, while one would be able to image any area by squinting, it is unlikely that the same image with the same squint would have been taken in previous passes. So, the imaging would be continuous, but not the

Table 1 (Color online) Requirements defined for Integrated Water Vapour (IWV) from WMO-OSCAR (<http://www.wmo-sat.info/oscar>). Note that, taking into account the density of liquid water, the IWV expressed in kg/m² is equivalent to the total Precipitable Water (PWV) expressed in mm of liquid water [19]*

Id	Variable	App area	Uncertainty (kg·m ⁻²)	Horizontal resolution (km)	Observation cycle	Timeliness	Coverage
380	Integrated water vapour (IWV)	High res NWP	1	0.5	15 min	15 min	Global
			2	5	60 min	30 min	
			5	20	6 h	2 h	
449	Integrated water vapour (IWV)	Nowcasting/VSRF	1	5	15 min	5 min	Global
			2	10	30 min	10 min	
			5	50	60 min	30 min	

* Goal is marked blue, breakthrough orange and threshold red.

Table 2 (Color online) Requirements defined for soil moisture for hydrometeorological and hydroclimatological applications, see also [27]*

Id	Variable	App area	Uncertainty (m ³ /m ³)	Horizontal resolution (km)	Observation cycle	Timeliness	Coverage
222	SM at surface	GEWEX	0.01	15	24 h	10 d	Global land
			0.02	50	3 d	15 d	
			0.05	250	10 d	30 d	
301	SM at surface	Global NWP	0.02	5	3 h	3 h	Global land
			0.04	15	1 d	1 d	
			0.08	100	5 d	5 d	
377	SM at surface	HI res. NWP	0.02	1	1 h	0.5 h	Global land
			0.04	5	3 h	3 h	
			0.08	40	6 h	6 h	

* Goal is marked blue, breakthrough orange and threshold red.

interferometric imaging. Instead, if the synthetic antenna position stays the same, as it happens in the GeoSTARe or MIMO solutions, the interferometric image taken say 12 h before is available at any time. Thus, the GeoSTARe or MIMO solutions only, that scan the same synthetic antenna and are not strip mapping, provide continuous interferometry everywhere.

A competing method to measure the PWV is the use of dense Global Navigation Satellite System Networks (GNSS), that allows the continuous extraction of the columnar water vapor [23, 24] and also yields some tomographical information coming from the slanting paths. However, the spatial resolution is lower, first because all the available GNSS satellites are considered with different viewing angles so that the troposphere delay is averaged on a surface of about 7 km diameter [25]. Then, the size of the available mesh of modern GNSS network is of the order of say 10 km or much more. Thus, geosynchronous systems of the GeoSTARe or MIMO type reach in a few minutes the aperture length needed for a say 1 km azimuth resolution, that is still much higher than that reachable with a reasonable ground based network.

The soil moisture is another parameter that could be studied using the interferometrical phase shifts induced by moisture itself. In fact, we read from [26] that soil moisture changes can be evaluated from the non triangularity of three interferometric phase readings of a soil in three passes. Current WMO requirements highlight the need for higher temporal resolution than current SAR sensors—see Table 2.

It is important to observe that in both cases i.e. both for the PWV and the soil moisture, the acceptable spatial resolution could be of the order of 1 km or even lower. In the case of PWV, though, the temporal updating rate is relevant, and we shall see that it can be very small, say a few minutes in the case that the observation point does not change with time and therefore the coherence is expected to be high. As said, this would not happen for higher eccentricities or higher inclinations because then the coherence would be lost due to the different squint angles to be used at different times of the day to achieve visibility from different locations in orbit. Furthermore, achieving the sensitivity needed in Table 2 is a tough task for a geosynchronous (or geostationary) SAR, needing very high power in L (or maybe C) band.

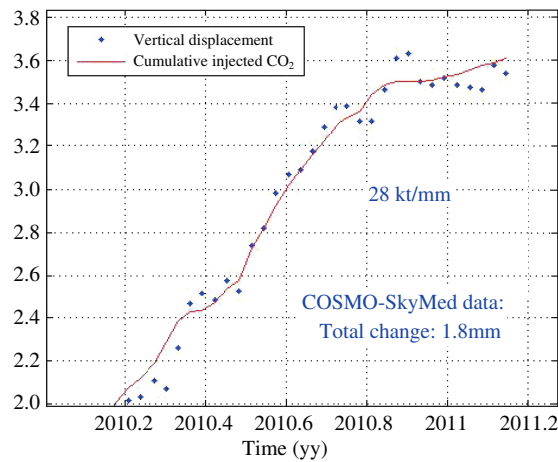


Figure 6 (Color online) Time series of the ground motion for a CO₂ injection site in Algeria, together with the injected volumes [28]. The height scale is significant.

4 Measuring ground motion

As well known, interferometric measurements yield ground motion with remarkable spatial resolution with a quality to the millimeter, see Figure 6. This is true as long the motion is not aliased, in that more than a quarter wavelength distance (due to the two way travel path) is covered along the LOS, between two successive passes. This is acceptable in the cases of subsidence of the terrain and for single events like in co-seismic motion, and leads to useful results. Notice that the average revisit time of those constellations that are available today, such as COSMO-SkyMed or Sentinel 1, is of the order of 2 and 3 days respectively, counting ascending and descending orbit passes. However, immediately after an earthquake, many other ground motions follow in a very short time, so that it would be very useful to be able to measure them, in Near Real Time. In this case, the continuity of a geosynchronous system would be very welcome, again using aperture scanning rather than strip mapping.

Further, also a rich constellation in a near equatorial orbit, like the 10° inclination in reference [29], could lead to short interferometric revisit times, up to say 6–8 h. Notice that using multiple swaths or squints these times could be reduced, but then non coherent views should be accepted. But then again, in order to have an interferometric survey, one would need the second image to be taken under the same angle. Hence, strip map systems, geosynchronous or not, would be able to yield the result only during the repeat passes, whereas stationary antenna scan systems like GeoSTARe or Argos would be able to trade resolution and revisit time to kilometers and tens of minutes.

5 Observing infrastructures

The ground motion due to subsurface excavations, mining, oil extraction can be sizeable and could go up to millimeters or more per day. Notice that if this motion exceeds 10 cm per day, than the long time T_{eq} of Geostare like systems (120 days) would be damaging, as the moving object would shift in azimuth more than a resolution cell. In the case of infrastructure works, controls by terrain leveling are often done daily, so that only daily or more often than daily observations could supersede in full this kind of activity, see [30]. In these cases, a very high target coherence can be expected. During this very short time of revisit, not only L and C bands, but also X and Ku band radars achieve interferometric coherences that allow very high precision measurements of the LOS displacement, even on distributed scatterers.

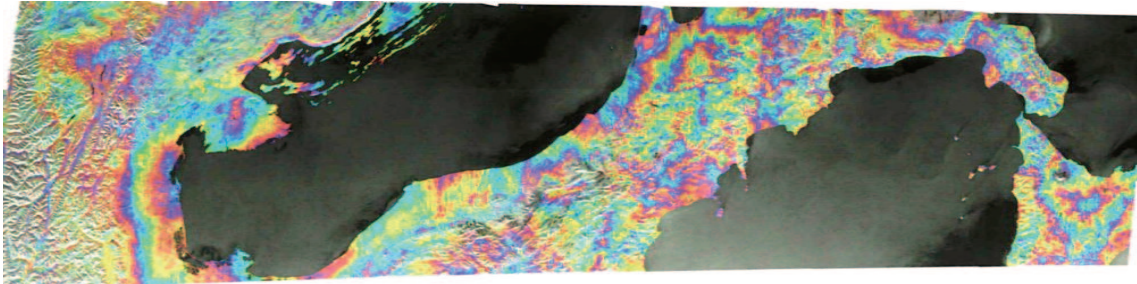


Figure 7 (Color online) Sentinel-1 Interferogram over Italy: repeat pass 12 days (1 and 13 March 2015). Fringes represents mostly differential water vapor.

6 Detecting changes

All the different solutions to the geosynchronous SAR's share the possibility of twice daily revisit and full resolution. In the case of change detection, low resolution images would be close to worthless, and thus full resolution images are needed, see Figure 7. Then, the complete antenna extent has to be covered, and therefore comparisons can be made only once daily (or twice, in the case that the return pass of the orbit coincides or it is close enough to the forward one, so that most of the image spectrum is shared). However, it is mandatory to observe that the changed ground will only be visible after the “dust has settled”, that is, only if there is no further change during the data gathering. In that case the clutter would at least partially affect the image, making the change detection much more difficult.

7 Disturbances and link budget

7.1 Atmospheric phase screen

Targets in motion while being imaged are not only defocused, but are also imaged far away from their azimuth position as if they moved at the LOS velocity for the time T_{eq} that could be hours or even months. So, only resting targets can be imaged: but then, the ever changing Atmospheric Phase Screen might attribute them a motion that would lead to the loss of the image [31, 32]. Hence, this effect has to be corrected. For one, the well expectable change of the two way water vapor delay of say 1 cm in a two hours-time would move the target hundreds of meters in the case of systems that scan a stationary synthetic antenna. The simple solution, to be adopted necessarily in the case of scanned antennas, is to measure low resolution interferograms say every 15 min, exactly those that would be useful to measure the PWV, and then use them to correct for the APS phase shift. As the resolution increases with time, the solution cannot be completely satisfying, as there will be always some uncorrected residual due to local PWV changes. However, the result appears to be sufficient to guarantee interesting results even during daylight (night atmospheres are usually much more quiet), and reasonable results even for violent phenomena.

7.2 Clutter

From what has been seen, moving targets are strongly defocused and thus create noise everywhere in the image. Hence, the amount of moving targets in an image has to be evaluated in order to establish the effects of their clutter. While the effects of the APS changes are independent of the wavelength, the clutter is dependent on that. In fact, considering the interferometric images taken 12 days apart by Sentinel 1²⁾, it is visible that the coherence is reasonably high and therefore most of the energy in C band—see Figure 7—and even more so in L band will remain in place. Thus, the amount of clutter will be significant but not prohibitive [14]. As lower frequencies imply wider antennas or lower resolution, studies on what happens in X and Ku band are mandatory. Billingsley [33] created a model for clutter as

2) http://www.esa.int/spaceinimages/Images/2015/06/Italy_interferogram.

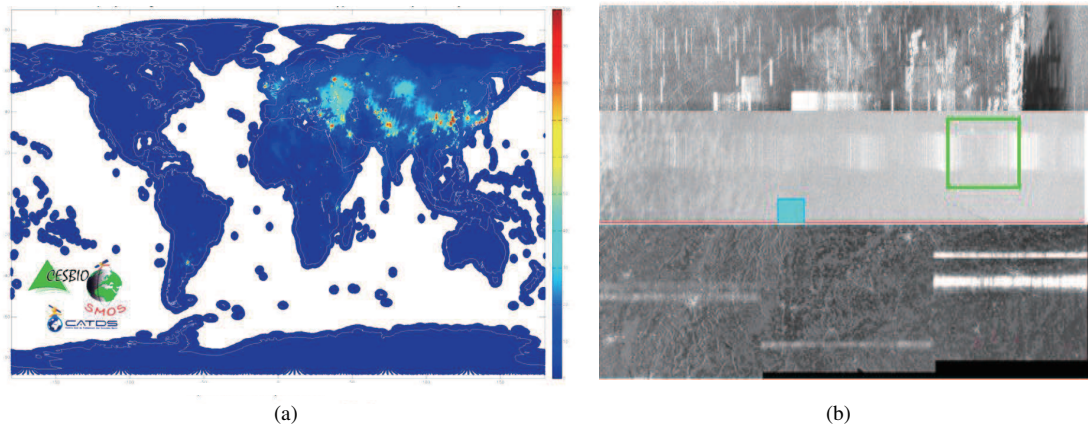


Figure 8 (Color online) (a) RFI observed by SMOS: such global maps are available from CESBIO http://www.cesbio.ups-tlse.fr/SMOS_blog/smos_rfi/; (b) examples of RFI observed in C-band.

a function of frequency, but this model, that was tested on time scales of the order of seconds, does not necessarily work for the much longer time scales, minutes and hours, needed for the scanned antennas and also for the strip map systems.

Experiments have been carried out [14] that show that even for X band, the clutter, much better during night time, is not prohibitive. The anyway significant noise floor abates increasing the number of looks and using temporal filtering, thus making even this band quite interesting. On the other hand, both C as well as L band are much better conditioned from the clutter viewpoint.

7.3 Interferences

A careful analysis should be carried out to monitor Radio Frequency Interferences (RFI), that may harm GEO-SAR much more than any LEO SAR, considering that the 40 times increase of distance from Earth cannot be compensated by a 40×40 increase in antenna directivity (hence area). The whole Earth is seen within 18° from a geosynchronous orbit and any jammer could disturb a GEO-SAR.

Let us introduce first the question of the passive interferences. Examples of L and X band interference measured from LEO Satellites are shown in Figure 8. The typical integration time of a LEO SAR is in the order of a second and scales to minutes, for the geosynchronous, and hours, for the geostationary. Therefore, not only the amplitude of Radio Frequency Interferences (RFI) will be magnified by (at least) 20 dB, but many of them would be incoherently added in the wide antenna footprint. An accurate scan of the existing interferences should be carried out before initiating the design of any such a system. In C band meteorological radars would impair the view [34]. In L band significant interferences have been measured by radiometers, like Soil Moisture and Ocean Salinity (SMOS), and Aquarius, scatterometers and also L band radars, like the Advanced Land Observation Satellite (ALOS) [28,29]. Even in X band—where the primary service is ESS-Active (Earth Exploration Satellite Service), there may be problems, though antennas are much more directive than in the other cases. Nonetheless, the RFI level has to be studied say using as receivers the radar satellites that are available today. In the future, one could take advantage of NASA cubesat mission CubeSat Radiometer Radio Frequency Interface Technology (CubeRRT), that plans to test techniques designed to mitigate RFI at higher frequencies—particularly in the 6 to 40 GHz range.

Moreover, GEO-SAR power illuminates a huge swath, say $700 \text{ km} \times 700 \text{ km}$, that is hundreds of times the typical Sentinel-1 LEO-SAR, $250 \text{ km} \times 5 \text{ km}$. This means that any LEO-SAR, and imagers in general (SAR, altimeters, scatterometers, wind profilers) causes a backscatter much stronger than GEO-SAR and possibly interfering in the same bandwidth. Figure 9 shows the typical illumination of Sentinel-1 in 12 h and 4 d, superposed to the 1-way footprint of an hypothetical 5 m antenna in C band placed at the geostationary orbit.

One has not only to consider LEO-SAR as source of passive interferences, but any other active sensors,

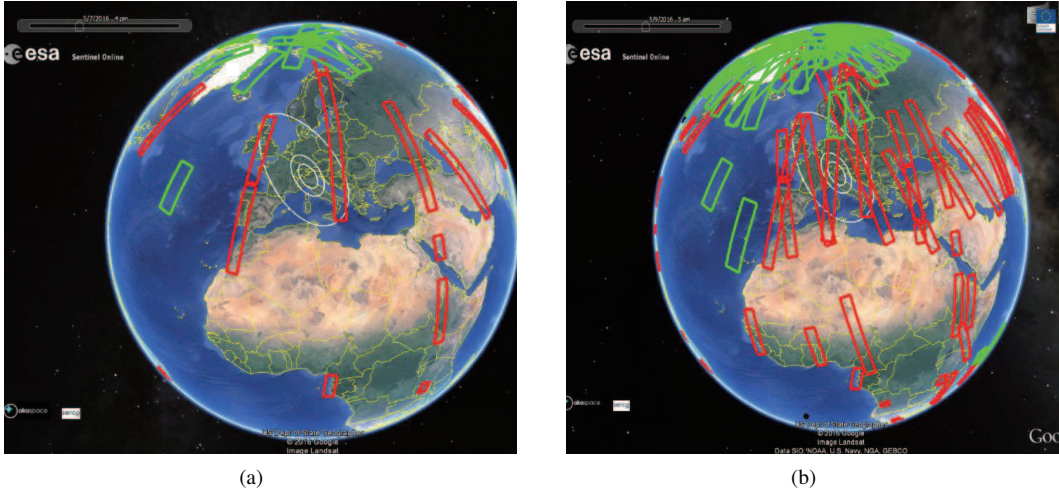


Figure 9 (Color online) Typical Sentinel1-A acquisitions in 12 h (5/8/2016 3 am–3 pm) (a) and in 4 days (b), superposed to a 5 m C-band antenna 1-way patterns -3 , -10 , -25 dB. Red and green defines the Wide and Extra Wide Swath modes respectively, with coverage 250 and 400 km.

be they scatterometers, altimeters, wind-profilers radars, etc. They would impact in two ways: with the direct illumination from the side-lobes of the transmitters antennas, (and maybe spurious leakage from the back of the satellite), and with the radiation backscattered from the ground.

The first objection to this type of interference would be that these satellites would illuminate only for short time intervals and thus they could be notched out by the geosynchronous system, just renouncing to that time interval. Further, as the remote sensors are mostly dawn dusk the interference sources would be present only along the solar terminator, that slides with the passage of time along the imaged area. It would be reasonable to synchronize the passage of the terminator with the time intervals correspondent to the extremes of the orbit, when the apparent satellite velocity is low, so that there would be enough time to recover the interfered data. This would also be convenient as the night and day time intervals behave in a widely different way in terms of tropospheric and ionosphere disturbances.

True, but notice that the large field of view of the geosynchronous satellites would always encompass some of them, for sure with the antenna side-lobes. So, at the moment, MIMO like solutions appear to be preferable from this viewpoint, as they could easily combine the data from the different phase centers to achieve adaptive notching in given directions in range and azimuth, with relatively small losses on the main beam.

Anyway, this appears to be a significant problem worth being studied carefully.

Further, we have to consider the active interferences. In the case of the scanned antennas, this could be seen as a misuse of the available spectrum, as a continuous signal would be always present in the background. Again, this is material worth being studied in cooperation with the international agencies that regulate the spectrum usage.

8 The link budget

The link budget is [12]

$$\frac{\eta P_t G}{4\pi R^2} \frac{\delta_{az} \delta_{range}}{\sin \alpha} \sigma_0 \frac{A_{ric}}{4\pi R^2} \frac{T_{obs}}{N_0} = \text{SNR}, \quad (2)$$

where η are total losses, P_t the average transmitted power, G the antenna gain, α the incidence angle, δ_{az} , δ_{range} the two spatial resolutions, σ_0 the value for σ_0 , A_{ric} the area of the receiver's antenna, N_0 the noise power spectrum density and finally T_{obs} the observation time and Signal to Noise Ratio (SNR) the signal to noise ratio.

We can rephrase (2) by isolating the contribution of the transmitted power, the observation time and

the resolution cell size, A_{res} (the term in the second fraction), assuming all the other terms as constant:

$$P_t \cdot T_{\text{obs}} \cdot A_{\text{res}} = \text{SNR} \cdot \frac{(4\pi R^2)^2 N_0}{\eta \sigma_0 A_{\text{ric}} G} = 250 \text{ W} \times 8 \text{ h} \times 10 \text{ m} \times 10 \text{ m}, \quad (3)$$

where the rightmost term has been evaluated in GeoSTARe case by assuming a range 38000 km, a backscatter -14 dB, 4 dB total losses, noise power spectrum of -202 dB_W and a 5 m antenna diameter with 1.4 illumination losses. The SNR has been assumed 6 dB at the beam center, that corresponds ~ 0 dB at the edge of the antenna footprint, that is roughly $750 \text{ km} \times 400 \text{ km}$.

In the geosynchronous case, the typical 2 min image time demands for a factor 460, that can be divided between the antenna size, 25 m, and a mean power 10 times larger, that is 2 kW.

We can furthermore exploit (1), for GeoSTARe, to derive performances in terms of sensitivity in water-vapor maps estimation. The standard deviation in the Integrated Water Vapor can be related to the standard deviation of the interferogram phase as from [17]:

$$\sigma_{\text{IWV}} = \Pi \cdot \sigma_{\varphi} \frac{\lambda}{4\pi} \cos \alpha = \Pi \cdot \frac{1}{\sqrt{\text{SNR} \cdot N_L}} \frac{\lambda}{4\pi} \cos \alpha, \quad (4)$$

where $\Pi \sim 0.15$ is the conversion from path delay to water vapor and N_L is the number of looks. In 15' the resolution cell is $320 \text{ m} \times 10 \text{ m}$ giving $N_L \sim 700$ looks in $0.5 \text{ km} \times 0.5 \text{ km}$ IWV resolution cell, and then $\sigma_{\text{IWV}} = 0.08 \text{ mm}$, that is well within the most restrictive ‘‘goal’’ in the user needs in Table 1.

9 Proposed solutions for continuous Earth observation

9.1 Inclined and eccentric geosynchronous SAR’s

The inclined Geosynchronous Earth Orbit Synthetic Aperture Radar was firstly proposed in [1]. Many recent studies have been carried out by the Chinese research community to improve the performances of the early geosynchronous concepts. Three types of orbits are recommended, such as two types of ‘figure-8’ orbits, and one ‘figure-O’ orbit. The geosynchronous system would have the agile range looking pointing ability from $\pm 2.2^\circ$ to $\pm 7.4^\circ$ through adjusting the feed pointing, along with the capability of the right/left looking and the forward/backward squint looking of a maximum of 60° by rotating the platform. These designs can greatly enhance the revisit and real time monitoring ability. The system would employ a large reflective antenna with 26 m diameter. The required averaged transmitting power is around 2 kW (Noise Equivalent Sigma Zero, NESZ, -20 dB) [5, 8, 9].

In the case of Telecom Compatible solutions, namely GeoSTARe [11], the almost fixed position in orbit allows for continuous interferometric observations that in turn allows trading image time for resolution. The long integration time allows moderate power resources and makes this concept suited for being hosted on telecommunication satellites. In that case, the orbit box of $\pm 0.1^\circ$ leads to a maximum eccentricity of $8e - 4$, a synthetic aperture in the order of σ of 140 km and a fine azimuth resolution in the range from 4 m (X band) to 30 m (L band). The orbit maintenance is not demanding, mainly needing a compensation of the longitude drift. One of the major limitations of the entire concept is the incidence angle that increases with latitude, covering the range from 40° to 70° corresponding to central Europe. The coverage at north is impaired by the long shades. Nonetheless, the compatibility with COMMunication SATellites ensures the availability of near ubiquitous users satellite television antennas as targets of opportunities.

9.2 MIMO: fractioned system in GEO-stationary orbit

This proposal [18, 19] advocates an innovative observing system that is unique in achieving instantaneous, continental-scale access, and less than hourly revisit, whilst keeping resolution as fine as a LEO SAR. It comprises a fractioned swarm of N neighboring geostationary compact SARs, all receiving not only their own signal (monostatic) but also the signals from the other radars (bistatic), and eventually, M other light satellites to be used as receivers only. A bistatic radar is approximately equivalent to a monostatic

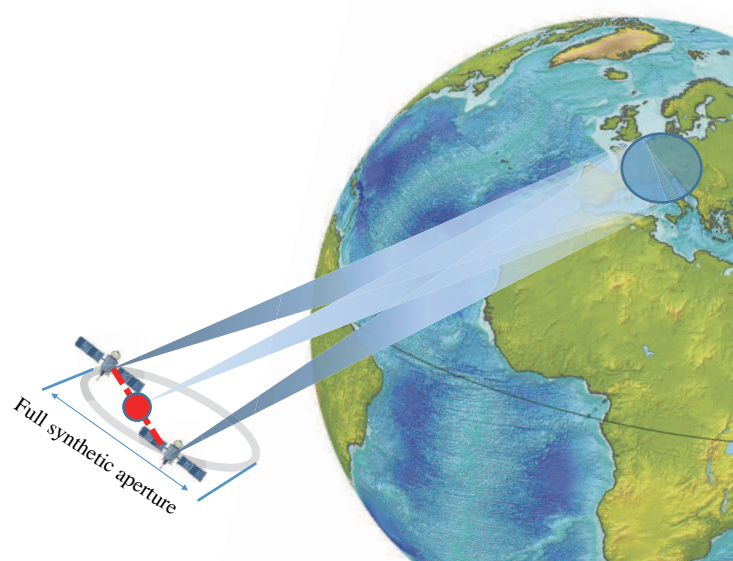


Figure 10 (Color online) Representation of a swarm made by two real satellites and one virtual, the bistatic phase center, corresponds to the red dot. The satellites follows each other on the same elliptical orbit.

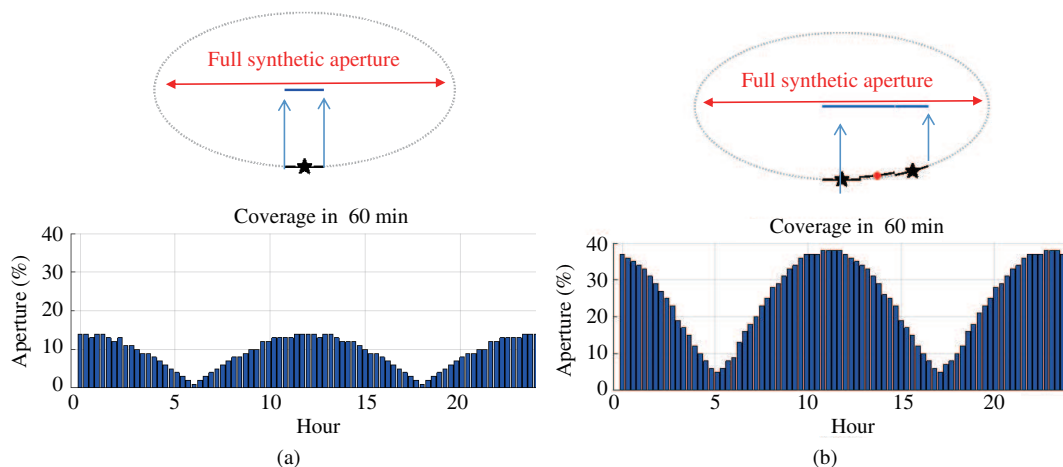


Figure 11 (Color online) Comparison between a single GEO-SAR (a), and a swarm of two GEO-SARs in bistatic configuration (b). Upper panels: Earth Centered Earth Fixed tracks of the real (black star) and virtual (red dot) phase centers. Lower panel: percentage of the full aperture covered in one hour, at different times of the day.

one positioned mid-way between source and receiver [25]. Then, using two radars generates a third, virtual observation, using three radars six observations, etc. Such quadratic scaling with the elements that is revolutionizing radar is called MIMO radar [20]. Hence, $N_c = N \times (N + 1)/2 + N \times M$ equivalent monostatic radars are made available in different positions along the equatorial orbit. This allows a progressive scan of a real 100 km wide antenna, to be completed in a fraction of the time needed to a single satellite, say $12/N_c$ hours, while keeping the interferometric global access.

The observation potential results from such a short image time, combined with the factor $N \times (N + M)$ improvement of the link budget, that fully exploits the fractioned power of the N transmitters and the fractioned receiving antenna of the $N + M$ receivers.

A simple example can be provided just by two mini-satellites in the same orbit, leading to three phase centers as shown in Figure 10.

One possible configuration is placing them so that the orbit is repeated after one hour, as shown in Figure 11, that is a multistatic extension of GEMINI [35]. The percentage of the full aperture covered

in one hour is also shown in the barplot of the figure for different times, and compared with the single satellite case.

That constellation achieves an interferometric revisit time of one hour with a synthetic aperture that ranges from 5% to 35% of the full one (covered within 12 h), whereas the single satellite gets 12 h revisit time with a synthetic aperture ranging from 0 to 12% in one hour.

Reducing the interferometric time from 12 h back to 1 h is maybe the most relevant achievement of the swarm. This in turn would ensure high correlation even in X band, and maybe in even higher frequencies, keeping the high sensitivity to deformations and atmospheric phase screens, combined with a very good SNR and resolution-enhanced by the use of the MIMO.

9.3 LEO constellations

It is worth to evaluate the dimensions of LEO or MEO constellations capable of achieving similar results. We first start with observing that no system, apart from MIMO, can achieve fully resolved interferometric imaging in minutes for all visible locations. GeoSTARe achieves low resolution continuous interferometric imaging but it is more affected by clutter and by the impact of the extremely long equivalent time.

From any given instant, all strip map systems need to wait on the average 6 h (for the twice daily pass) to get a new image, if interferometric coherence is considered to be necessary. If interferometry is not required, and if all squints are acceptable, then the delay to the change detection would be just that of the time needed to create an antenna T_{ant} , or T_{obs} . This would be a few minutes for [1], whereas for the lower inclination strip map systems the delay would be say twice as much. Hence, change detection is well insured by all geosynchronous systems, and it would even be interferometric in the MIMO case, whereas the others systems would need up to 6 h, on average, to achieve this capability. Notice, that for strip map and GeoSTARe systems, the scene has to be stationary again to avoid unacceptable defocusing.

A LEO constellation capable of being in view (non interferometric) of say all the Earth below 45° latitude within a delay of a few minutes would consist of L satellites, that we now suppose having both left and right view. Supposing very optimistically that at height 800 km the incidence angle could go from 20° to 50° , then each satellite might control two strips each say 500 km wide and therefore, at a ground velocity of say 7 km/s, it would cover an area of about $7000 \text{ km}^2/\text{s}$. As all the area below 45° is about 350 Million km^2 , then a world wide coverage at that latitudes would require 50000 [satellites \times seconds]. To achieve the visibility in $20'$, more than 35 satellites would be needed at 800 km height, even with all the satellites being in a near equatorial orbit! Sure enough, increasing the delay time to 2 h, the number would reduce 6 fold to say 6 satellites: notice that the latitudes off the equator would be much better served. To have interferometry, we could consider a 3 days revisit cycle, with about 500 km distance between successive descending or ascending equator crossings. With 12 satellites, one would get interferometric surveys anywhere within 6 h, on average. At the optimal height of 3000 km [4] the area covered per unit time would be much larger. However, the systems to be used would likely be much more complex. Considering a 1 day revisit and 9 orbits per day, one would get 6 h average interferometric revisit time adopting 2 satellites. So, the result would now be similar to the strip map geosynchronous solutions, with the added advantage of a much shorter T_{eq} . LEO and MEO solutions would thus allow ship traffic monitoring.

From these observations we see that, in order to achieve hourly observations, the geosynchronous orbit increases the efficiency of the satellite of a factor between 6 and 10. The weakest points of this solution are the sensitivity to interferences, briefly discussed in a previous section, and the incapability of observing objects in motion.

10 Summary and conclusion

Table 3 summarizes the considerations made up to now, referring to 12.5 m spatial resolution. It appears that each solution has its own interest; however, as new problems might come out from the experiments, it appears advisable to start experimentations with the least expensive solutions.

Table 3 (Color online) Comparison between geosynchronous and LEO MEO configurations

Solution	Band	Image revisit	Clutter	T_{ant}	T_{obs}	T_{eq}	SNR	RFI	Size	Moving targets
Tomiyasu	L	daily	Medium	2'	Low	6 h	Good	High	Large	No
Strip map	L	daily	Low	7'	Low	14 h	Good	Medium	Large	No
Geostare	C	minutes	Medium	7 h	High	120 d	Medium	High	Small	No
Argos	X	minutes	Low	20'	Low	0	Good	Good	Medium	No
LEO	X	days	Low	1 s	Low	2'	Good	Good	Medium	Yes
MEO	X	1 day	Low	3 s	Low	11'	Good	Medium	Medium	Yes

The conclusion that can be drawn from the preceding exposition is that indeed geosynchronous systems are the least complex solution to achieve continuous observations. Systems in MEO or LEO would need far more satellites to obtain the 12 h not to speak of the 2 h or even 20' delay obtainable with GEO solutions.

For one, a single X band system of say 1 ton mass and 5 m on board antenna would scan the 100 km synthetic antenna in less than 12 h then achieving in this time interferometric i.e. coherent change detection capabilities with a 5 m resolution. However, a single satellite would be quite sensitive to the changes of the atmospheric phase screen. A couple would do much better, reducing of a factor 2 the observation time (factor 3 in the case of bistatic use), and achieving a much safer compensation of the phase shifts. The MIMO solution appears to be the most appropriate in the long term. In the case of C band, a 1 ton satellite would suffice, as it would be less sensitive to the APS; in exchange, the resolution would halve to 10m. An L band system would be more complex and heavy. It would be more performing in terms of time of observation, reducible to minutes, but it would be more sensitive to ionosphere. The delay of coherent observation would still be 12 h.

None of the geosynchronous systems, even in their most complex realisation (Tomiyasu or MIMO) could for now achieve moving targets observations—unless their motion is predictable—as their random motion of many wavelengths in the at least 2' observation time would not allow coherent focusing. However, new promising work [36] or some extreme version of compressive sensing or data adaptivity may be able to solve this problem, for now still unsolved.

Conflict of interest The authors declare that they have no conflict of interest.

References

- Tomiyasu K, Pacelli J L. Synthetic aperture radar imaging from an inclined geosynchronous orbit. *IEEE Trans Geosci Remote Sens*, 1983, GE-21: 324–329
- Madsen S, Edelstein W, DiDomenico L D, et al. A geosynchronous synthetic aperture radar; for tectonic mapping, disaster management and measurements of vegetation and soil moisture. In: *Proceedings of IEEE International Geoscience and Remote Sensing Symposium*, Sydney, 2001. 1: 447–449
- Prati C, Rocca F, Giancola D, et al. Passive system reusing backscattered digital audio broadcasting signals. *IEEE Trans Geosci Remote Sens*, 1998, 36: 197
- Edelstein W N, Madsen S N, Moussessian A, et al. Concepts and technologies for synthetic aperture radar from MEO and geosynchronous orbits. *Proc SPIE*, 2005, 5659, doi: 10.1117/12.578989
- Hu C, Li Y H, Dong X C, et al. Optimal data acquisition and height retrieval in repeat-track geosynchronous SAR interferometry. *Remote Sens*, 2015, 7: 13367–13389
- Hu C, Li Y H, Dong X C, et al. Performance analysis of L-band geosynchronous SAR imaging in the presence of ionospheric scintillation. *IEEE Trans Geosci Remote Sens*, 2017, 55: 159–172
- Dong X C, Hu C, Tian Y, et al. Experimental study of ionospheric impacts on geosynchronous SAR using GPS signals. *IEEE J Sel Top Appl Earth Observ Remote Sens*, 2016, 9: 2171–2183
- Zhang Q J, Gao G T, Gao W J, et al. 3D orbit selection for regional observation GEO SAR. *Neurocomputing*, 2014, 151: 692–699
- Hu C, Long T, Zeng T, et al. The accurate focusing and resolution analysis method in geosynchronous SAR. *IEEE Trans Geosci Remote Sens*, 2011, 49: 3548–3563
- Hu C, Tian Y, Yang X P, et al. Background ionosphere effects on geosynchronous SAR focusing: theoretical analysis and verification based on the BeiDou navigation satellite system (BDS). *IEEE J Sel Top Appl Earth Observ Remote Sens*, 2016, 9: 1143–1162

- 11 GeoSTARe. ESA contract N 40001085494/13/NL/CT. Study on utilisation of future telecom satellites for Earth observations. 2013
- 12 Monti Guarnieri A, Bombacib O, Catalanob T F, et al. ARGOS: a fractioned geosynchronous SAR. *Acta Astronaut*, 2015. In press
- 13 Monti Guarnieri A, Broquetas A, Recchia A, et al. Advanced radar geosynchronous observation system: ARGOS. *IEEE Geosci Remote Sens Lett*, 2015, 12: 1406–1410
- 14 Recchia A, Monti Guarnieri A, Broquetas A et al. Impact of scene decorrelation on geosynchronous SAR data focusing, geoscience and remote sensing. *IEEE Trans Geosci Remote Sens*, 2016, 54: 1635–1646
- 15 D’Aria D, Leanza A, Monti-Guarnieri A, et al. Decorrelating targets: models and measures. In: *Proceedings of IEEE International Geoscience and Remote Sensing Symposium (IGARSS)*, Beijing, 2016. 3194–3197
- 16 Recchia A, Monti Guarnieri A, Belotti M, et al. Demonstrative geosynchronous SAR products affected by clutter and APS decorrelation. In: *Proceedings of IEEE International Geoscience and Remote Sensing Symposium (IGARSS)*, Milan, 2015. 1265–1268
- 17 Pichelli E, Ferretti R, Cimini D, et al. InSAR water vapor data assimilation into mesoscale model MM5: technique and pilot study. *IEEE J Sel Top Appl Earth Observ Remote Sens*, 2015, 8: 3859–3875
- 18 Wadge G, Monti Guarnie A, Hobbs S E, et al. Potential atmospheric and terrestrial applications of a geosynchronous radar. In: *Proceedings of IEEE International Geoscience and Remote Sensing Symposium*, Québec, 2014. 946–949
- 19 Bevis M, Businger S, Chiswell S, et al. GPS meteorology: mapping zenith wet delays onto precipitable water. *J Appl Meteorol Climatol*, 1994, 33: 379–386
- 20 Sato K, Realini E, Tsuda T, et al. A high-resolution, precipitable water vapor monitoring system using a dense network of GNSS receivers. *Journal Disaster Res*, 2013, 8: 37–47
- 21 Cheng S L, Perissin D, Lin H, et al. Atmospheric delay analysis from GPS meteorology and InSAR APS. *J Atmos Sol-Terr Phys*, 2012, 86: 71–82
- 22 Bock Y, Wdowinski S, Ferretti A, et al. Recent subsidence of the Venice Lagoon from continuous GPS and interferometric synthetic aperture radar. *Geochem Geophys Geosyst*, 2012, doi: 10.1029/2011GC003976
- 23 Perler D. Water vapor tomography using global navigation satellite systems. Dissertation for the Doctoral Degree. Swiss Federal Institute of Technology Zurich, 2011. <http://dx.doi.org/10.3929/ethz-a-006875504>
- 24 Awange J. *Environmental Monitoring using Global Navigation Satellite Systems*. Berlin/Heidelberg: Springer-Verlag, 2012
- 25 Onn F, Zebker H. Correction for interferometric synthetic aperture radar atmospheric phase artifacts using time series of zenith wet delay observations from a GPS network. *J Geophys Res*, 2006, 111, doi:10.1029/2005JB004012.
- 26 De Zan F, Zonno M, López-Dekker P, et al. Phase inconsistencies and water effects in SAR interferometric stacks. In: *Proceedings of Fringe 2015 Workshop*, Frascati, 2015
- 27 Entekhabi D, Njoku E G, O’Neill P E, et al. The soil moisture active passive (SMAP) mission. *Proc IEEE*, 2010, 98: 704–716
- 28 Rocca F, Rucci A, Ferretti A, et al. Advanced InSAR interferometry for reservoir monitoring. *First Break*, 2013, 31: 77–85
- 29 M. L’Abbate, Germani C, Torre A, et al. Compact SAR and micro satellite solutions for Earth observation. In: *Proceedings of 31st Space Symposium on Technical Track*, Colorado, 2015
- 30 Ferretti A. *Satellite InSAR Data: Reservoir Monitoring from Space (EET 9)*. EAGE Publications, 2014
- 31 Bruno D, Hobbs S. Radar imaging from geosynchronous orbit: temporal decorrelation aspects. *IEEE Trans Geosci Remote Sens*, 2010, 48: 2924–2929
- 32 Belotti M, Broquetas A, Leanza A, et al. An efficient method for the azimuth compression of geosynchronous SAR data through sub-apertures processing. In: *Proceedings of IEEE International Geoscience and Remote Sensing Symposium (IGARSS)*, Melbourne, 2013. 2047–2050
- 33 Lombardo P, Greco M, Gini F, et al. Impact of clutter spectra on radar performance prediction. *IEEE Trans Aerosp Electron Syst*, 2001, 37: 1022–1038
- 34 Rodon J R, Broquetas A, Monti Guarnieri A, et al. Geosynchronous SAR focusing with atmospheric phase screen retrieval and compensation. *IEEE Trans Geosci Remote Sens*, 2013, 51: 4397–4404
- 35 Guarnieri A M, Tebaldini S, Rocca F, et al. GEMINI: geosynchronous SAR for Earth monitoring by interferometry and imaging. In: *Proceedings of IEEE International Geoscience and Remote Sensing Symposium*, Munich, 2012. 210–213
- 36 Chen X L, Guan J, Huang Y, et al. Radon-linear canonical ambiguity function-based detection and estimation method for marine target with micromotion. *IEEE Trans Geosci Remote Sens*, 2015, 53: 2225–2240